

Orbit spectral density versus stimulus identity and intensity

Andy G. Lozowski^{a)}

*Department of Electrical and Computer Engineering, Southern Illinois University Edwardsville,
Edwardsville, Illinois 62026, USA*

(Received 25 February 2008; accepted 18 July 2008; published online 18 August 2008)

A concept of orbit spectral density for a one-dimensional iterated function is presented. To compute orbit spectral density, a method of extracting low-order periodic orbits from the dynamical system defined by the iterated function is first used. All points of the dynamics are then partitioned among the periodic orbits according to a distance measure. Partition sizes estimate the density of trajectories around periodic orbits. Assigning these trajectory densities to the orbit indexes introduces the orbit spectral density. A practical computational example is presented in the context of a model olfactory system. © 2008 American Institute of Physics. [DOI: [10.1063/1.2969069](https://doi.org/10.1063/1.2969069)]

Traditionally in nonlinear system analysis, researchers focus not only on signals but also on dynamical systems that produce the signals. From this point of view, signals are trajectories in the phase space and dynamical systems can be characterized by the contents of their phase space. For the sake of analyzing neural spiking signals, we propose a method to create a dynamical system from signal realizations. The dynamical system is a one-dimensional iterated function in metric space. We inspect the phase space of the system for the presence of recurrent points by tracking backward trajectories. As a result, we find all periodic orbits up to a given order and use them as centers to partition the phase space according to the metric. We introduce the term orbit spectral density, which is a mapping of the periodic orbits onto the size of their partitions. Trajectory density distribution in the phase space is reflected in the orbit spectral density. This characterizes signals using the orbit spectrum in metric spaces, much as the Fourier magnitude spectrum characterizes signals in linear spaces.

Neural signals by their nature are sequences of spikes distributed in time. It is possible to assume that the information, carried by neural signals, is in the time intervals between the spikes and not their magnitudes or shapes. Applying this assumption may, in reality, introduce some information loss. However, processing of the information that is still retained becomes a simpler task.

Another assumption can be made about some neural signals to further simplify the task. In the case of sensory neurons, the neurophysiological evidence suggests a lack of temporal coding other than simple temporal modulation with the stimulus intensity. In other words, the order in which the intervals are found in the spiking sequence is not an essential feature. All of the information can be compiled into an interval probability distribution function. Its parameters will depend on the type and intensity of the stimulus.

We introduce a concept of orbit spectral density to quantify the interval distribution density of a neural signal. The goal is to provide a suitable signal analysis tool that could be used as one of the methods to classify the information embedded in neural signals. The construction of orbit spectral density will be presented through an example application to analyze the identity and intensity of odorant mixes in a model olfactory system.

OLFACTORY SYSTEM MODEL

In biological neural networks, most sensor neurons perform a very simple function. Their role is to detect an input stimulus and react to varying intensity of the stimulus. Neurons produce spikes at their output encoding the information in a straightforward fashion: the more stimulus is delivered to the sensor neuron, the more frequent is its output firing.

In mammalian olfactory systems, the input stimulus is delivered by odorant molecules depositing in the mucus inside the nasal cavity. The right kind of odorant molecules can reach sensory neurons embedded in the epithelium causing them to fire. The probability of a sensory neuron firing is related to the number of stimulant molecules. In general, the average time interval between the neural spikes decreases with the increase of the stimulant concentration. At a certain concentration level, sensory neurons experience saturation. This is when the interspike intervals can no longer decrease because of the refractory limitation. This determines the interspike interval minimum.

Another neurophysiological observation is that the deviation of the interspike intervals as measured at the sensory output is related to the stimulus concentration as well. Concentrated scents will invoke frequent firing with little deviation in time distance between the spikes. Low concentrations of the stimulus, however, cause more spread to the firing intervals up to the point of a complete lack of regularity in the neural activity of the sensor.

Many experimental approaches were based on response measurements and fitting of concentration-response curves to data. Typically, the average interspike interval of the olfactory receptors has an asymptotic dependency on the stimulus

^{a)}Electronic mail: a.lozowski@ieee.org.

intensity. We shall use an approximation method introduced in Ref. 1. In this study, various odorants including camphor (A), limonene (B), and isoamyle acetate (C) were inspected for the relationship as to how the odorant concentration affects the firing rate of sensory neurons. Using a change of variables defined in Ref. 2, the firing rate is represented by the average interspike intervals $\langle\tau\rangle$, whereas the odor intensity is converted to the odor sparsity s . The odorant sparsity s is the amount of air used to dissolve 1 mol of the substance. Coordinates (τ, s) are approximately linearly related to each other,

$$\langle\tau\rangle = \tau_0 + Gs. \quad (1)$$

The minimum interval τ_0 and temporal modulation gain G are constant parameters specific to a given sensor type. Using the measurement data presented in Ref. 1, parameters τ_0 and G are calculated for the three example odorants:

	Camphor (A)	Limonene (B)	Isoamyle acetate (C)
G	$0.18 \frac{\text{ms}}{\text{MI/mol}}$	$0.71 \frac{\text{ms}}{\text{MI/mol}}$	$4.8 \frac{\text{ms}}{\text{MI/mol}}$
τ_0	80 ms	130 ms	100 ms

Equation (1) represents temporal modulation of interspike intervals in the sensor response. This effect is common in a class of neural sensors broader than just mammalian olfactory system.³

Details of the workings of the olfactory system are not completely known. However, it is clear that the sensory information distributed among a myriad of olfactory sensors is represented in a much compacted way further down the biological signal processing channel. We will present here one such method of representing temporally modulated spiking distributions.

First, we adopt the Maxwell distribution to describe spiking activity of the neural sensor for a given odorant type. Maxwell distribution has a suitable threshold to represent the minimum spiking interval τ_0 . Moreover, both the average value and variance depend on the same parameter σ . Therefore, by making $\sigma = \sqrt{\pi/8}(\tau_0 + Gs)$, the average interspike interval $\langle\tau\rangle$ and the interval deviation relate to the odorant sparsity s , just as introduced earlier on. The resulting interval distribution is defined by the following equation:

$$p(\tau) = \frac{1}{\sigma^3} \sqrt{\frac{2}{\pi}} (\tau - \tau_0)^2 \exp\left(-\frac{(\tau - \tau_0)^2}{2\sigma^2}\right). \quad (2)$$

As shown in Fig. 1, diluting the odorant in more air decreases the resolution of the sensor responses by spreading the interspike intervals over a broader range of values. Having more spread causes the average to shift toward larger values since the lower bound on τ is fixed.

Living organisms perceive odors as sensations caused by mixtures of odorant molecules. Therefore, in any modeling attempt, it is essential to consider more than one type of stimulus at a time. Various odorant molecules excite different groups of receptors. A superposition of these excitations constitutes the odor as detected by the olfactory bulb.⁴ For the sake of simplicity, we assume that individual excitations con-

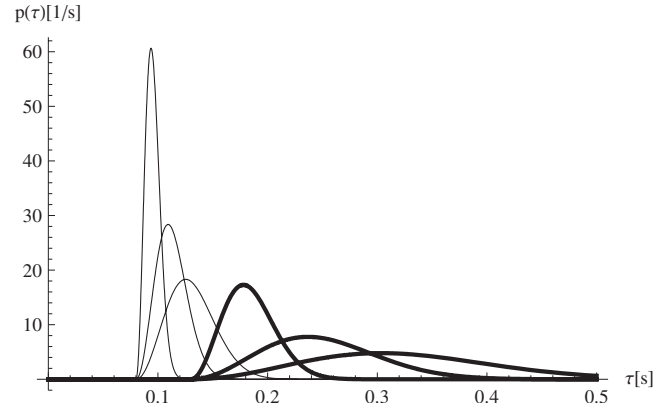


FIG. 1. The interspike interval distribution $p(\tau)$ of a sensor neuron depends on the odorant sparsity s . Two odorants, A (thin line) and B (bold line), are shown at three sparsity levels: 100, 200, and 300 MI/mol (left to right).

tribute to the superposition in proportion to their intensities. The relative concentrations of individual components constitute the odor identity, whereas the absolute concentrations determine the odor intensity.

ORBIT SPECTRAL DENSITY

With the help of a computer, a realization of the interspike interval sequence can be obtained from a given interval distribution function. A sufficiently large amount of computer-generated data will adequately represent the interval distribution. Suppose A is a finite set of intervals generated from the distribution associated with odorant A. In the same manner, let B and C be finite sets generated from odorant B and C distributions, respectively. We represent a mix of odorants by the union of sets $A \cup B \cup C$. The relative concentrations of odorants in the mix are reflected by ratios of set cardinalities $|B|/|A|$ and $|C|/|A|$. An example realization of 1000 interspike intervals synthesized for a mix of (0.2, 0.5, 1) mol of odorants A, B, and C is shown in Fig. 2. The plot is a random permutation of 118 points generated from odorant A distribution, 294 points generated from distribution B, and 588 points from C.

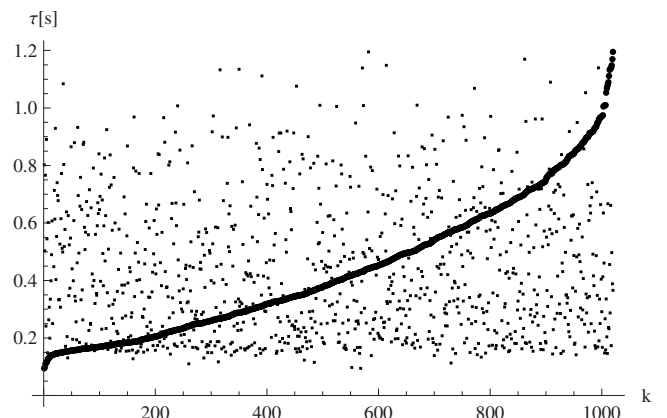


FIG. 2. A 1000 point realization of interspike intervals generated for a mix of (0.2, 0.5, 1) mol of odorants A, B, and C diluted in 100 MI of air. Corresponding ordered sequence $\text{sort}(A \cup B \cup C)$ shown in bold.

We will use the term ordered sequence for a realization of an odorant or a mix of odorants. For odorant A, ordered sequence $a: \{1, 2, \dots, |A|\} \rightarrow A$ is derived from the realization as $a = \text{sort}A$, where the ordering operator sort is a simple sorting $\forall_{i,j} i < j \Rightarrow a_i < a_j$. For a mix of odorants, ordered sequence $r: \{1, 2, \dots, |A \cup B \cup C|\} \rightarrow A \cup B \cup C$ is derived from the union $r = \text{sort}(A \cup B \cup C)$ in the same manner.

The ordered sequence can be used to estimate the cumulative distribution function in ergodic systems. In Fig. 2, the shape of the overall cumulative distribution function can be inferred by interpolating the graph. The ordered sequence is a very extensive, hence impractical representation of odorant mix realizations. Instead, we propose using a dynamical system to describe a rule of generating realizations of odorant mixes. In order to define a dynamical system, let us again generate a large mix of interspike interval realizations using the same system of interval distribution functions. Let A' , B' , and C' be the sets of intervals corresponding to odorants A, B, and C, respectively. Again, the ordered sequence $r': \{1, 2, \dots, |A' \cup B' \cup C'|\} \rightarrow A' \cup B' \cup C'$ is derived.

We now define support for our dynamical system to be a set $\Omega = A \cup B \cup C \cup A' \cup B' \cup C'$. This is simply a set of all intervals generated by the computer so far. Set Ω forms a complete metric space with a finite number of elements and the standard metric inherited from the real line. Let $q: \{1, 2, \dots, |\Omega|\} \rightarrow \Omega$ be the ordered sequence derived from the support as $q = \text{sort}\Omega$. Elements of this sequence are mapped back into Ω according to the following transformation $T: \Omega \rightarrow \Omega$:

$$T = \{(q_k, r_k): 1 \leq k \leq |A \cup B \cup C|\} \cup \{(q_{k+|A \cup B \cup C|}, r'_k): 1 \leq k \leq |A' \cup B' \cup C'|\}. \quad (3)$$

Transformation T is in fact a union of two monotonic branches T_0 and T_1 , represented by the two terms in Eq. (3). Formally, $T_0 = T|_{T^{-1}(A \cup B \cup C)}$ and $T_1 = T|_{T^{-1}(A' \cup B' \cup C')}$.

Transformation T will be iterated to generate trajectories $\tau_{i+1} = T(\tau_i)$ in space Ω . The domain of T is rather coarse. Nevertheless, we will be seeking low-order recurrent points with property $T^N(\tau) \approx \tau$ and $1 < N \leq |\Omega|$. Such points can be very efficiently found by tracking reverse iterations $T(\tau_{n+1}) = \tau_n$. Every reverse iteration must select either branch T_0 or T_1 , for uniqueness. Let us index the two branches of T with address $\alpha_n \in \{0, 1\}$. We are seeking N -periodic solutions, therefore N -periodic address sequences are needed: $\alpha_{n+N} = \alpha_n$. Since cardinalities of domains $\text{dom}T_0$ and $\text{dom}T_1$ are less than $|\Omega|$, the inverse branch mappings need to be extended to cover the missing points. This will be done using the nearest neighbor in the domain for approximation,

$$\tilde{T}_0^{-1}(\tau_n) = \tau_{n+1} \in \text{dom}T_0: |\tau_n - T_0(\tau_{n+1})| = \min_{\tau} |\tau_n - T_0(\tau)|, \quad (4)$$

$$\tilde{T}_1^{-1}(\tau_n) = \tau_{n+1} \in \text{dom}T_1: |\tau_n - T_1(\tau_{n+1})| = \min_{\tau} |\tau_n - T_1(\tau)|.$$

As shown in Fig. 3, starting with an initial condition τ_1 and $(\alpha_1, \alpha_2, \dots, \alpha_N)$, reverse trajectory τ_n converges to an N -periodic orbit while iterating

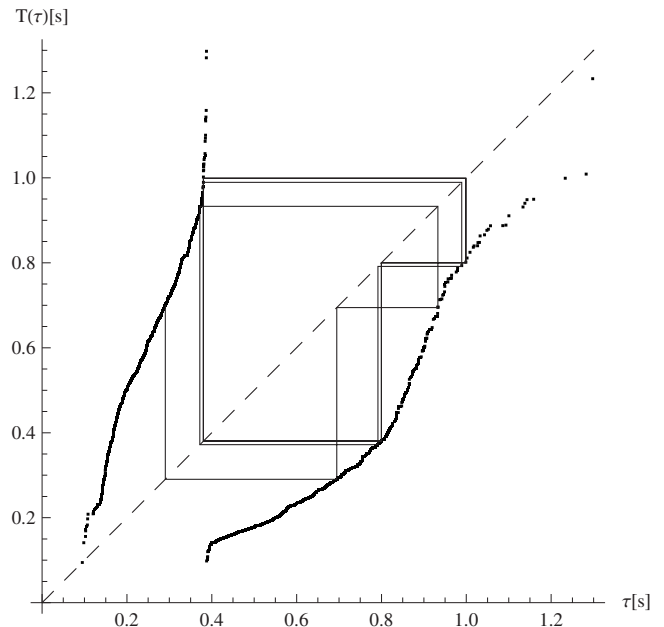


FIG. 3. Transformation $T: \Omega \rightarrow \Omega$ combines two distinct monotonic branches T_0 (left) and T_1 (right). Convergence of iterated operation $T_1^{-1} \circ T_0^{-1}$ from the initial condition $\tau_1 = 0.7s$, extracting periodic orbit $(0, 1, 1)$ shown.

$$\tau_{n+1} = \tilde{T}_{\alpha_n}^{-1}(\tau_n). \quad (5)$$

Note that with probability 1, both \tilde{T}_0^{-1} and \tilde{T}_1^{-1} are contraction mappings. According to Banach's fixed point theorem, for a given address α , trajectories generated by iterations (5) converge to the same periodic orbit regardless of the initial condition τ_1 . Thus, the orbit address α solely defines the orbit trajectory. In Table I, addresses of all distinguishable orbits of period 2, 3, 4, and 5 are listed.

Our overall goal is to provide a basis for characterization of various odorant mixes. Using low-period orbits of a dynamical system offers the advantage of being independent of the details of the receptor spiking activity. The orbits are identifiable by their address. Their realizations are derived from the interspike interval distributions and allow for defining orbit spectral density, for a given realization of interval

TABLE I. Periodic orbits of a two-branch transformation up to the order $N=5$.

Orbit	Address α
ξ_1	(0,0,0,0,1)
ξ_2	(0,0,0,1)
ξ_3	(0,0,0,1,1)
ξ_4	(0,0,1)
ξ_5	(0,0,1,0,1)
ξ_6	(0,0,1,1)
ξ_7	(0,1)
ξ_8	(0,1,0,1,1)
ξ_9	(0,1,1)
ξ_{10}	(0,0,1,1,1)
ξ_{11}	(0,1,1,1)
ξ_{12}	(0,1,1,1,1)

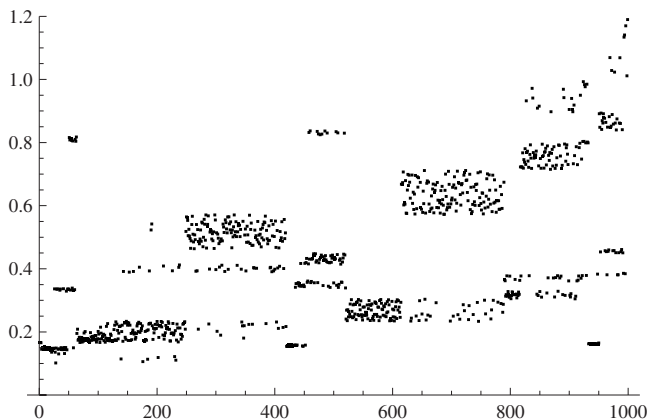


FIG. 4. A 1000 point realization of interspike intervals generated for a mix of (0.2,0.5,1) mol of odorants A, B, and C diluted in 100 ML of air. The intervals are partly ordered with respect to closeness to orbits shown in Table I.

sequence. Each odorant mix corresponds to a different orbit spectrum. The odor identity and intensity information can be deduced from the spectrum, which will be the primary application of the idea.

Let us consider a single orbit ξ , one of the orbits included in Table I. In the set of all intervals $A \cup B \cup C$ shown in Fig. 2, some of the intervals are going to be closer to orbit ξ than to any other orbit from the table. The distance of an interval to the orbit is understood as the minimum of the distances to the solutions of Eq. (5). Let expression $(A \cup B \cup C)|_{\xi}$ denote the set of all intervals in $A \cup B \cup C$ closest to orbit ξ . The realization of the interval distribution in Fig. 2 is now partitioned among all orbits and organized according to sequence $\xi_1, \xi_2, \dots, \xi_{12}$, which is shown in Fig. 4. The subsequence of points from Fig. 2 falling into partition ξ_1 is now shown first, then subsequence for ξ_2 , and so on. Every orbit occupies certain windows in the interval value space. Some orbits are more prevalent than others.

Expressing distribution density of orbits rather than individual intervals will prove more effective in describing odorant mixes. The simplest orbit (0,1) from the orbit set is selected as a fundamental orbit to serve as the density reference. All other orbits can be assigned their relative densities as

$$W(\xi) = \frac{|(A \cup B \cup C)|_{\xi}}{|(A \cup B \cup C)|_{(0,1)}}. \quad (6)$$

Number $W(\xi)$ describes the contribution that orbit ξ has in the total density of interval realizations. Therefore, W may be regarded as an orbit spectrum and serve as a representation of the underlying distribution features.

In Fig. 5, three odorant mixes are compared in terms of their orbit spectral densities. The first and the last mix are distinctly different odors. We expect the spectra to reflect this difference by comparing each orbital component. This indeed is the case.

The middle odorant mix is a composition of the first and the last one shown. Inspecting the spectra, the middle one seems to combine the features of the other two. This property

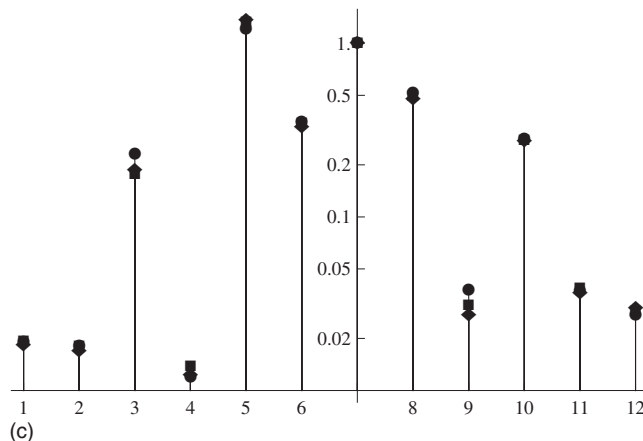
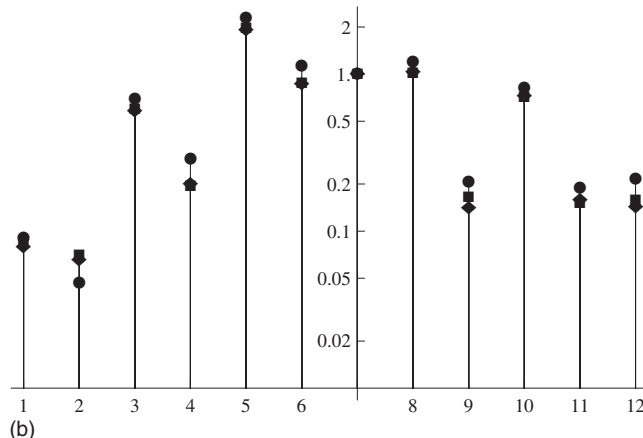
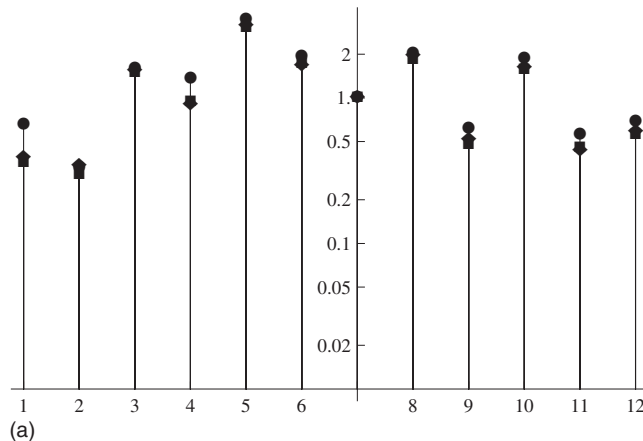


FIG. 5. Orbit spectral densities $W(\xi)$ of three odorant mixes: (0.3,0.5,2) (top), (0.25,0.5,1.5) (middle), and (0.2,0.5,1) (bottom). Each mix comes in three sparsity levels: 100 (circle), 200 (square), and 300 ML/mol (diamond).

of the orbit spectrum may prove useful in decrypting the chemical structure of unknown mixes of known components.

Lastly, the orbit spectrum appears to preserve its integrity under various concentration levels. A change of concentration is definitely detectable, but the entire pattern of the spectrum remains identifiable.

There are synchronization systems in which oscillators are coupled in a network to perform various information processing tasks. When storing information as unstable periodic oscillations,⁵ such systems do not lock trajectories on a periodic orbit. Instead, the system trajectory visits vicinities of

orbits corresponding to stored bits of information according to the stimulus driving the network. The orbit spectrum would be a natural way to represent the information retrieval process in such dynamic behavior. The olfactory cortex is one of the examples of actual biological systems where stimulus-driven synchronization is found.⁶

Orbit spectral density may be used to formulate synchronization of dynamical systems that are physically different but have similar topological properties. In Ref. 7, synchronization of coupled uniform piecewise linear Markov maps was considered. About 10^{13} of such maps are possible all with the same distribution density of points but different time realizations. Synchronization of such systems is detectable by comparing their invariant density measures. The same can be accomplished by comparing their orbit spectra instead.

FINAL REMARKS

There are other ways to derive a single-dimensional transformation from data, such as those in Ref. 8. In contrast to other methods, we have restricted our mathematical apparatus to a minimum remaining within the concept of metric spaces. The main advantage of such an approach is that the represented quantities do not need to be elements of a linear space. In the context of the example olfactory system, the model scents are not vectors. Instead, we represent them as trajectories of a dynamical system in a metric space. In metric spaces, it is natural to describe each pair of scents with a

non-negative number related to a measure of how close one scent resembles the other. More importantly, in metric spaces the existence of scents cancelling other scents, or even the existence of a zero scent, is not required. This fits well with the fact that sensory neurons will fire even if no odorant molecules are present.

Orbit spectral density is akin to the magnitude of the Fourier spectrum, which is used extensively to analyze signals in Hilbert spaces. Decomposition of neural signals into low-periodic trajectories resembles the description of signals with their harmonic components. We expect the identity of odors be present in such a decomposition. At the same time, diluting the odors in air is a feature suppressed in the orbit spectrum. That resembles suppression of phase shifts in the Fourier magnitude spectrum.

¹J. P. Rospars, P. Lansky, P. Duchamp-Viret, and A. Duchamp, *BioSystems* **58**, 133 (2000).

²A. G. Lozowski, M. Lysetskiy, and J. M. Zurada, *IEEE Trans. Neural Netw.* **15**, 1268 (2004).

³R. W. Friedrich and G. Laurent, *Science* **291**, 889 (2001).

⁴T. A. Dickinson, J. White, J. S. Kauer, and D. R. Walt, *Trends Biotechnol.* **16**, 250 (1998).

⁵P. Thiran and M. Hasler, *Int. J. Circuit Theory Appl.* **24**, 57 (1996).

⁶W. J. Freeman, *Int. J. Bifurcation Chaos Appl. Sci. Eng.* **2**, 451 (1992).

⁷M. Hasler, in *Proceedings of the 1997 IEEE International Symposium on Circuits and Systems*, Hong Kong (IEEE, Piscataway, NJ, 1997), pp. 1045–1048.

⁸D. Pingel, P. Schmelcher, and F. K. Diakonou, *Chaos* **9**, 357 (2000).